

Nanowaveguides and couplers based on hybrid plasmonic modes

Jie Tian, Zhe Ma, Qiang Li, Yi Song, Zhihong Liu et al.

Citation: *Appl. Phys. Lett.* **97**, 231121 (2010); doi: 10.1063/1.3524515

View online: <http://dx.doi.org/10.1063/1.3524515>

View Table of Contents: <http://apl.aip.org/resource/1/APPLAB/v97/i23>

Published by the [American Institute of Physics](#).

Related Articles

Waveguide-integrated near-infrared detector with self-assembled metal silicide nanoparticles embedded in a silicon p-n junction

Appl. Phys. Lett. **100**, 061109 (2012)

On-chip single photon emission from an integrated semiconductor quantum dot into a photonic crystal waveguide

Appl. Phys. Lett. **99**, 261108 (2011)

Critical optical coupling between a GaAs disk and a nanowaveguide suspended on the chip

Appl. Phys. Lett. **99**, 151117 (2011)

Low-loss polymer waveguides on nanoporous layers

Appl. Phys. Lett. **99**, 153301 (2011)

Low-loss polymer waveguides on nanoporous layers

APL: Org. Electron. Photonics **4**, 216 (2011)

Additional information on *Appl. Phys. Lett.*

Journal Homepage: <http://apl.aip.org/>

Journal Information: http://apl.aip.org/about/about_the_journal

Top downloads: http://apl.aip.org/features/most_downloaded

Information for Authors: <http://apl.aip.org/authors>

ADVERTISEMENT

NEW!

iPeerReview

AIP's Newest App



Authors...
Reviewers...

Check the status of
submitted papers remotely!

AIP | Publishing

Nanowaveguides and couplers based on hybrid plasmonic modes

Jie Tian,¹ Zhe Ma,² Qiang Li,¹ Yi Song,¹ Zhihong Liu,³ Qing Yang,² Chaolin Zha,¹ Johan Åkerman,^{1,4} Limin Tong,² and Min Qiu^{1,2,a)}

¹School of Information and Communication Technology, Royal Institute of Technology (KTH), 16440 Kista, Sweden

²Department of Optical Engineering, State Key Laboratory of Modern Optical Instrumentation, Zhejiang University, Hangzhou 310027, People's Republic of China

³Department of Materials Science and Engineering and State Key Laboratory of Silicon Materials, Zhejiang University, Hangzhou 310027, People's Republic of China

⁴Department of Physics, University of Gothenburg, 41296 Gothenburg, Sweden

(Received 31 May 2010; accepted 3 November 2010; published online 10 December 2010)

Experimental demonstration of silicon nanowires based hybrid plasmonic waveguides and couplers with subwavelength mode confinement at the near infrared wavelength $\lambda=980$ nm are presented. By measuring the radiating light from the discontinuities in a nanowire, the estimated propagation length of the hybrid plasmonic waveguide is about $30 \mu\text{m}$ (corresponding to a propagation loss of $\sim 0.14 \text{ dB}/\mu\text{m}$). For the coupler, the experimental results show that the hybrid plasmonic modes can be efficiently coupled between two overlapping nanowires only with a $1.9 \mu\text{m}$ long coupling length. © 2010 American Institute of Physics. [doi:10.1063/1.3524515]

Recently, many studies have been focused on the down-scaling of the optical device, which is a critical issue in modern information industries. Different efforts for reducing the size of the circuits elements have been proposed and demonstrated using structures such as silicon chip waveguide elements,¹⁻³ planar photonic crystals devices,⁴⁻⁷ and semiconductor nanowires^{8,9} *et al.* However, the miniaturization and the high-density integration of such optical devices under half optical wavelength scales are obstructed by the light diffraction limitation. A promising approach to circumvent this problem is to exploit the surface plasmon modes, which are light waves coupled to free electron oscillations in a metal that can be laterally confined below the diffraction limit using subwavelength metal structures.¹⁰⁻¹² Many different functional plasmonic devices have been developed and demonstrated experimentally, such as V-shape groove channel waveguide components,¹³ nanometal particle waveguides,¹⁴ metal nanowire waveguide elements,¹⁵⁻¹⁷ plasmonic waveguide lasers,¹⁸ high efficiency tapered couplers,¹⁹ and surface plasmon resonators based on crystalline gold microplates.²⁰ However, subwavelength mode confinement usually results in huge propagation loss at optical frequencies, which makes practical applications difficult, especially for nanometer scale photonic integration circuits based on plasmonic devices.^{21,22} For example, the light propagation length in a metal strip waveguide is typically around $2.5 \mu\text{m}$ (Refs. 23 and 24) and can only be increased to around $10 \mu\text{m}$ when using the very smooth surface of the chemically synthesized silver nanowires.^{25,26}

Recently, a theoretical study²⁷ predicted that a hybrid plasmonic waveguiding structure can significantly increase the propagation length while maintaining a strong subwavelength mode confinement. The simulation results showed that the surface plasmon polaritons can travel over large distances (e.g., $150 \mu\text{m}$) with subwavelength scale mode confinement (e.g., $\lambda^2/400$).²⁷ Later on, a deep subwavelength laser at a

wavelength of 489 nm was experimentally demonstrated by using such a hybrid plasmonic waveguiding structure, and the generated optical mode size is more than 100 times smaller than the diffraction limit.²⁸

In this letter, we demonstrate the experimental realization of such nanoscale hybrid plasmonic waveguides which confine light under the deep subwavelength scale at a near infrared wavelength (980 nm). In addition, we demonstrate a plasmonic nanodevice, hybrid plasmonic couplers, and investigate their optical properties. To the best of our knowledge, this work is the first experimental demonstration of subwavelength hybrid plasmonic waveguide guiding structures and functional nanophotonic devices at the near infrared wavelength, which represents a considerable advance toward the realization of nanoscale semiconductor-based plasmonic and photonics integration.

The schematic of the hybrid plasmonic waveguide structure is sketched in Fig. 1(a). Such a hybrid plasmonic waveguide consists of a high refractive index crystal silicon nanowire on a 70 nm thick silver surface, where a 13 nm thick silica layer is used to form the gap between the nanowire and the silver film [see the inset of Fig. 1(a)]. The gap layer between the semiconductor and the metal interface concentrates light into an extremely small subwavelength area. A

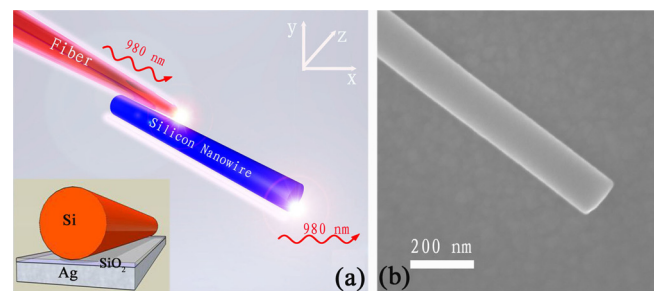


FIG. 1. (Color online) Nanoscale hybrid plasmonic waveguide. (a) The schematic of the plasmonic waveguide and its light in-coupling scheme. The inset is the cross section of the waveguide, showing the underlying layers. (b) The SEM image of a typical hybrid plasmonic waveguide.

^{a)}Author to whom correspondence should be addressed. Electronic mail: min@kth.se. Tel.: +46-8-790-4068. FAX: +46-8-790-4090.

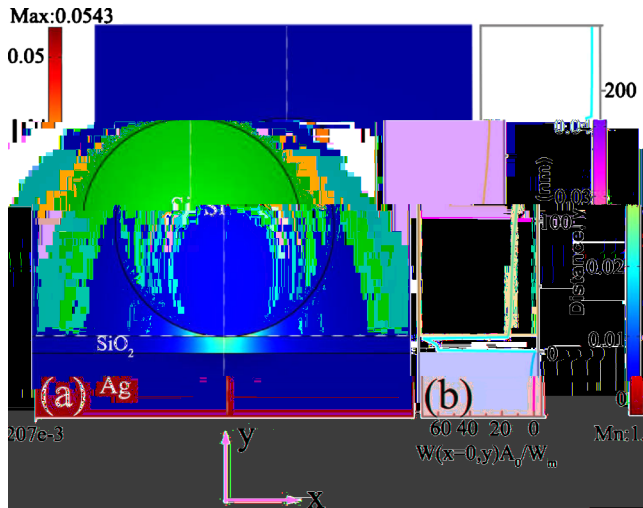


FIG. 2. (Color online) Hybrid plasmonic waveguide mode. (a) The calculated electric field distribution at the wavelength, $\lambda=980$ nm. Most of the energy is concentrated in the silica insulator layer. The diameter of the Si nanowire is 170 nm, SiO_2 thickness is 13 nm, and Ag thickness is 70 nm. $n_{\text{Si}}=3.625-0.00075i$ (Ref. 29), $n_{\text{SiO}_2}=1.45$, and $n_{\text{Ag}}=0.04-6.992i$ (Ref. 30) at the wavelength 980 nm. (b) Normalized energy density along the vertical dashed line in (a). $A_0=\lambda^2/4$. W is the electromagnetic energy distribution, and W_m is the total electromagnetic energy, respectively. The upper and bottom shaded areas represent silicon and silver regions, respectively.

scanning electron microscope (SEM) image of a silicon nanowire on the silver surface is shown in Fig. 1(b).

For a detailed analysis of the structure, we perform electromagnetic field simulations using the commercial finite-element package FEMLAB from COMSOL. Figure 2(a) illustrates the electromagnetic field distribution of the fundamental hybrid plasmonic mode, which shows that the mode is strongly confined in two dimensions within the gap. The electromagnetic energy density profiles in the gap are plotted in Fig. 2(b). The normalized mode area is $A_m/A_0=9.8 \times 10^{-3}$ (A_m and A_0 are the mode area in the waveguide and the diffraction-limited mode area,²⁷ respectively), which means the mode propagates within areas more than two orders of magnitude smaller than the diffraction-limited area in free space, $A_0=\lambda^2/4$. The calculated propagation length is 31 μm . The simulation results show that the photonic mode can also be excited so long as the nanowire diameter is above 185 nm. However, the photonic mode is x -polarized while the plasmonic mode is y -polarized.

The 70 nm silver film with a 5 nm adhesion titanium layer was deposited by the e-beam evaporation on a silicon substrate. Then a 13 nm thick silica layer covering the silver film was deposited at the room temperature using magnetron sputtering (ATC Orion-8). Single-crystalline silicon nanowires were fabricated by the chemical vapor deposition process.^{31–33} The plasmonic modes are excited by an evanescent coupling method.¹⁷ Laser light at the wavelength of 980 nm is coupled into a single mode fiber with a nanoscale tip at one end [Fig. 1(a)]. The fiber tip is placed in parallel and close contact with one end of the silicon nanowire, with an overlap length less than 1 μm . A microscope objective connected with a charge-coupled device camera is used to monitor that the plasmon mode is excited and capture the images of the plasmon mode transmitting along the waveguide.

A hybrid waveguide with a 12.5 μm long nanowire [170 nm in diameter, see Fig. 3(a)] is characterized first. The

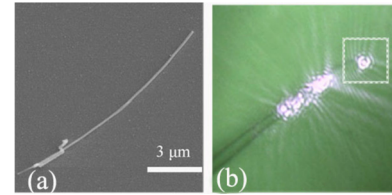


FIG. 3. (Color online) Hybrid plasmonic mode propagation in different waveguides. (a) SEM image of a 12.5 μm long nanowire (170 nm in diameter). (b) Optical microscope image illustrating the experimental excitation of the plasmonic mode in the waveguide.

bright light spot in the white square box in Fig. 3(b) clearly shows the light output from the nanowire end facet. Since the photonic mode is cut-off for the 170 nm diameter nanowire, we can conclude that the output is the plasmonic mode.

Then a hybrid plasmonic waveguides coupler is formed, as shown in Fig. 4. Figure 4(a) is the SEM image of the nanocoupler consisting of two silicon nanowires, where the lengths are 38 and 34 μm , and the diameters are 180 and 190 nm, respectively. The overlapping length is about 1.9 μm . The bright spots along the nanowire in Fig. 4(b) are the scattered light from the kinks, which can also be used to estimate the plasmonic wave propagation length. For the hybrid coupler, the excitation is from the down branch. The down branch has a diameter of smaller than 185 nm and thus only the plasmonic mode can be excited. In the experiment, a polarizer is used to control the polarization orientation of the input light. The output light intensity is maximized when the incident light is y -polarized. Through the directional coupling from the plasmonic mode in the down branch, only the plasmonic mode can be excited in the upper branch although the photonic mode can exist in the upper branch. As the propagation loss can be defined²⁴ as $I(x)=I_0e(-x/L_0)$, where I_0 is the initial intensity, x is the length of the nanowire in

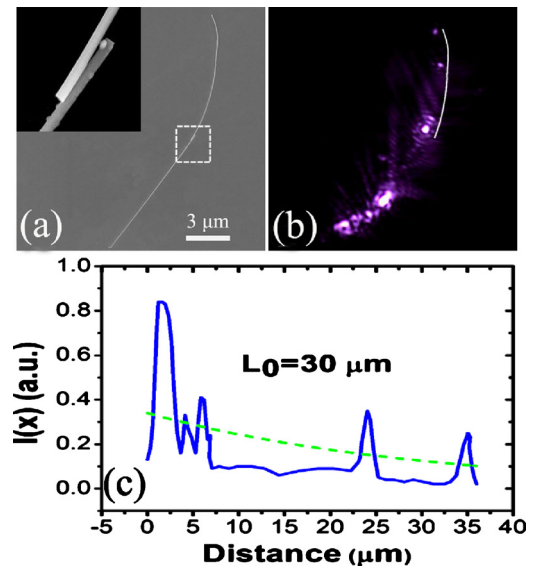


FIG. 4. (Color online) A hybrid plasmonic waveguide coupler. (a) SEM image of the coupler. The length of the lower waveguide is 38 μm and the diameter is 180 nm. The parameters are 34 μm and 190 nm for the upper waveguide. The overlapping part between two wires has a length of about 1.9 μm . Inset is the enlarged SEM image of the coupling area. (b) The dark field optical microscope image illustrates the propagation of light along the nanowire coupler. (c) Light density profile along the nanowire (white line direction) in (b). The dashed line is a fit of the data to an exponentially decaying function.

micrometers, and L_0 is the propagation length. In Fig. 4(c) we plot the intensity profile of light that emanated from the upper nanowire kinks, fitted with the above function. The approximate plasmonic wave propagation length is $L_0 = 30 \mu\text{m}$, which corresponds to a propagation loss of $0.14 \text{ dB}/\mu\text{m}$. For the coupling efficiency, the theoretical value is estimated to be as high as 70% and the experimental value is approximately 60%.¹⁵

Different materials absorptions contribute to the overall loss. For the 0.12 dB loss in $1 \mu\text{m}$ long waveguide, the absorptions in the silver and silicon account for 0.08 and 0.04 dB loss, respectively. The 0.02 dB extra propagation loss compared with the propagation loss measured from the experiment mainly originates from the scattering loss, which is caused by the imperfectly smooth silicon nanowire surface and the silver surface.

In conclusion, we have demonstrated the excitation and the propagation of subwavelength-scale plasmonic modes based on hybrid plasmonic waveguiding structures. Two different nanoscale photonic devices, such as waveguides and couplers, have been demonstrated and the optical properties have been characterized. Both simulations and experiments illustrate that the plasmonic mode can propagate in such hybrid waveguides with long propagation length. At the near infrared wavelength $\lambda = 980 \text{ nm}$, a propagation length of $30 \mu\text{m}$ (i.e., a propagation loss of $\sim 0.14 \text{ dB}/\mu\text{m}$) is obtained. For the coupler, an efficient light coupling with an only $1.9 \mu\text{m}$ long coupling part has been observed with two overlapping nanowires. These experimental demonstrations are essential steps for utilizing low loss nanowire based plasmonic components for high-capacity photonic integrated circuits.

This work is supported by the Swedish Foundation for Strategic Research (SSF), the Swedish Research Council (VR), and the National Natural Science Foundation of China (Grant No. 60728309). J.Å. is a Royal Swedish Academy of Sciences Research Fellow supported by a grant from the Knut and Alice Wallenberg Foundation. Qiang Li acknowledges the support from the China Scholarship Council.

¹Y. Vlasov, W. M. J. Green, and F. Xia, *Nat. Photonics* **2**, 242 (2008).

²M. A. Foster, R. Salem, D. F. Geraghty, A. C. Turner-Foster, M. Lipson, and A. L. Gaeta, *Nature (London)* **456**, 81 (2008).

³H. Yamada, T. Chu, S. Ishida, and Y. Arakawa, *IEEE Photonics Technol. Lett.* **17**, 585 (2005).

⁴Y. Tanaka, J. Upham, T. Nagashima, T. Sugiya, T. Asano, and S. Noda, *Nature Mater.* **6**, 862 (2007).

⁵L. H. Frandsen, P. I. Borel, Y. X. Zhuang, A. Harpøth, M. Thorhauge, M. Kristensen, W. Bogaerts, P. Dumon, R. Baets, V. Wiaux, J. Wouters, and S. Beckx, *Opt. Lett.* **29**, 1623 (2004).

⁶J. Tian, M. Yan, M. Qiu, C. R. Ribbing, Y. Z. Liu, D. Z. Zhang, and Z. Y. Li, *Appl. Phys. Lett.* **93**, 191114 (2008).

⁷B. Corcoran, C. Monat, C. Grillet, D. J. Moss, B. J. Eggleton, T. P. White, L. O'Faolain, and T. F. Krauss, *Nat. Photonics* **3**, 206 (2009).

⁸C. J. Barrelet, A. B. Greytak, and C. M. Lieber, *Nano Lett.* **4**, 1981 (2004).

⁹F. X. Gu, L. Zhang, X. F. Yin, and L. M. Tong, *Nano Lett.* **8**, 2757 (2008).

¹⁰W. L. Barnes, A. Dereux, and T. W. Ebbesen, *Nature (London)* **424**, 824 (2003).

¹¹J. B. Pendry, *Science* **285**, 1687 (1999).

¹²S. A. Maier, P. G. Kik, H. A. Atwater, S. Meltzer, E. Harel, B. E. Koel, and A. A. G. Requicha, *Nature Mater.* **2**, 229 (2003).

¹³S. I. Bozhevolnyi, V. S. Volkov, E. Devaux, J. Y. Laluet, and T. W. Ebbesen, *Nature (London)* **440**, 508 (2006).

¹⁴S. A. Maier, M. L. Brongersma, P. G. Kik, S. Meltzer, A. A. G. Requicha, and H. A. Atwater, *Adv. Mater.* **13**, 1501 (2001).

¹⁵A. L. Pyayt, B. Wiley, Y. Xia, A. Chen, and L. Dalton, *Nat. Nanotechnol.* **3**, 660 (2008).

¹⁶A. Manjavacas and F. J. G. Abajo, *Nano Lett.* **9**, 1285 (2009).

¹⁷X. Guo, M. Qiu, J. M. Bao, B. J. Wiley, Q. Yang, X. N. Zhang, Y. G. Ma, K. H. Yu, and L. M. Tong, *Nano Lett.* **9**, 4515 (2009).

¹⁸M. T. Hill, M. Marell, E. S. P. Leong, B. Smalbrugge, Y. Zhu, M. Sun, P. J. Veldhoven, E. J. Geluk, F. Karouta, Y. S. Oei, R. Nötzel, C. Z. Ning, and M. K. Smit, *Opt. Express* **17**, 11107 (2009).

¹⁹J. Tian, S. Yu, W. Yan, and M. Qiu, *Appl. Phys. Lett.* **95**, 013504 (2009).

²⁰B. J. Wiley, D. J. Lipomi, J. Bao, F. Capasso, and G. M. Whitesides, *Nano Lett.* **8**, 3023 (2008).

²¹G. Veronis and S. Fan, *Appl. Phys. Lett.* **87**, 131102 (2005).

²²M. A. Noginov, G. Zhu, M. Mayy, B. A. Ritzo, N. Noginova, and V. A. Podolskiy, *Phys. Rev. Lett.* **101**, 226806 (2008).

²³T. Yatsui, M. Kourogi, and M. Ohtsu, *Appl. Phys. Lett.* **79**, 4583 (2001).

²⁴L. Chen, J. Shakya, and M. Lipson, *Opt. Lett.* **31**, 2133 (2006).

²⁵A. W. Sanders, D. A. Routenberg, B. J. Wiley, Y. Xia, E. R. Dufresne, and M. A. Reed, *Nano Lett.* **6**, 1822 (2006).

²⁶Y. G. Ma, X. Y. Li, H. K. Yu, M. L. Tong, Y. Gu, and Q. H. Gong, *Opt. Lett.* **35**, 1160 (2010).

²⁷R. F. Oulton, V. J. Sorger, D. A. Genov, D. F. P. Pile, and X. Zhang, *Nat. Photonics* **2**, 496 (2008).

²⁸R. F. Oulton, V. J. Sorger, T. Zentgraf, R. M. Ma, C. Gladden, L. Dai, G. Bartal, and X. Zhang, *Nature (London)* **461**, 629 (2009).

²⁹E. D. Palik, *Handbook of Optical Constants of Solids* (Academic, New York, 1998).

³⁰P. B. Johnson and R. W. Christy, *Phys. Rev. B* **6**, 4370 (1972).

³¹J. Niu, J. Sha, X. Ma, J. Xu, and D. Yang, *Chem. Phys. Lett.* **367**, 528 (2003).

³²Y. Cui, L. J. Lauhon, M. S. Gudiksen, J. Wang, and C. M. Lieber, *Appl. Phys. Lett.* **78**, 2214 (2001).

³³See supplementary material at <http://dx.doi.org/10.1063/1.3524515> for the silica film, silver layer, and the silicon nanowire fabrication.